PROCEEDINGS, 45th Workshop on Geothermal Reservoir Engineering
Stanford University, Stanford, California, February 10-12, 2020
SGP-TR-216

Pulse Testing for Monitoring Aquifer Thermal Energy Storage

Peter A. Fokker[1,2,3], Eloisa Salina Borello[1], Dario Viberti[1], Francesca Verga[1] and Jan-Diederik van Wees[2,3]

[1] Politecnico di Torino, Turin, Italy

[2] TNO – Geological Survey of the Netherlands, Utrecht, The Netherlands

[3] Utrecht University, Utrecht, The Netherlands

peter.fokker@tno.nl

Keywords: Monitoring, Thermal Energy Storage, Well testing, Harmonic pulse testing

ABSTRACT

Geothermal energy systems often suffer the inefficiency resulting from the seasonally fluctuating demand between summer and winter. One possible solution is seasonal storage of heat in relatively shallow aquifers. However, the efficiency of such a system will depend on a number of factors that cannot all be known a priori. Thus the importance of monitoring. We have expanded our earlier work on harmonic pulse testing (HPT) to incorporate the effect of a temperature front moving into the reservoir due to injection of hot (or cold) water. To assess the feasibility of the technique for thermal front monitoring, we devised a synthetic field case where water at 90°C was stored in a 20°C aquifer. First, we employed a numerical reservoir simulator to determine the temperature distribution in a doublet system. Then, this distribution was imposed as initial condition for a pulse test simulated with the same numerical technique; in this way, synthetic data were created. The data was then analyzed using our new analytical relationships. The thermal front around the injector could indeed be characterized through the application of the proposed HPT interpretation methodology. A mobility change was detected around the injector, corresponding to an increased local temperature, approaching the injection value. Moreover, the estimated radius of the thermal front was in good agreement (within 10%) with the equivalent radius of the – not perfectly cylindrical – numerically calculated heated zone. Adding noise to the pressure data did not deteriorate the signal much, as long as the tests were carefully designed in terms of pulse duration and sampling rate.

1. INTRODUCTION

The development of Geothermal Energy in the Netherlands is mainly associated with heating. However, the seasonal swing of the climate and the daily fluctuations of the weather and of the heat demand make traditional geothermal doublets suboptimal: they cannot continuously operate at their optimal power. The economics of geothermal heat could therefore possibly be enhanced considerably by storage. One of the storage possibilities currently considered is seasonal storage of heat in shallow aquifers: ATES (Aquifer Thermal Energy Storage). It intends to store the surplus of energy supply in the summer and harvest it in the winter. This potentially increases the overall efficiency of the system. As an example, water of 80°C could be stored in an 80-m deep aquifer where the virgin temperature is only 20°C.

The efficiency of an ATES system critically depends on the ability to produce back the stored heat. This, in turn, depends on the distribution of reservoir properties and on the operational design. However, such knowledge is only partially available. The geological setting, including heterogeneities in the reservoir properties, cannot be completely known. Further, there will also be uncertainty about the resulting temperature distribution both after injection and after production. As a result, gaining knowledge of the heat distribution is key for being able to optimize the operational efficiency. It is thus obvious that there is a need for effective monitoring of the heat distribution upon injection and production of hot and cold water.

Well testing is an important technique for the determination of reservoir flow properties, including flow boundaries and mobility interfaces (Gringarten, 2008). Proper production/build up testing, however, requires a preliminary well shut-in to reach static pressure and a well shut-in during the build-up (Bourdet 2002). Moreover, to be interpretable, the registered pressure should not be influenced by activity in neighboring wells, thus a test usually involves also a temporary interruption of nearby operations. Harmonic pulse testing (HPT), on the contrary, is applicable during ongoing operations (Viberti et al., 2018) and does not require significant alteration of tested well net production/injection (Salina Borello et al., 2017). Furthermore, it does not require special equipment: the standard well testing equipment is sufficient, provided that well defined rate pulses are imposed and precise pressure monitoring is realized.

In the present contribution, we extend pulse testing methodology to the monitoring of thermal zones around a geothermal injector well or to the monitoring of a thermal energy storage system. After detailing the theoretical basis in the following section we will demonstrate the applicability of HPT to thermal front monitoring through the application of the developed analytical solution in the frequency domain for the interpretation of synthetic data generated adopting an in-house numerical model taking into account of thermal convection and conduction coupled with a commercial software for bottom hole pressure profile simulation accounting for noise. Then we will demonstrate the feasibility of the technique by creating synthetic measurements using a commercial numerical simulator, and by interpreting them with our analytical models. We close with a discussion of pitfalls and promises and some concluding remarks.

2. HARMONIC PULSE TESTING

The concept of Harmonic Pulse Testing was first proposed by Kuo (1972) and has since been developed for the determination of hydraulic parameters by several authors (Black & Kipp, 1981; Cardiff & Barrash, 2015; Despax et al., 2004; Hollaender, Hammond, & Gringarten, 2002), in different scenarios like two-phase flow (Fokker & Verga, 2011), fractured wells (Morozov, 2013; Vinci et al., 2015), fractured reservoir (Guiltinan & Becker, 2015), gas wells (Salina Borello et al., 2017), and horizontal wells (Fokker et al., 2018). It was also suggested for the characterization of heterogeneous reservoir (Ahn & Horne, 2010; Cardiff et al., 2013; Copty & Findikakis, 2004; Fokker et al., 2012; Rosa & Horne, 1997), fault hydraulic properties (Chen & Renner, 2018), and leakage from faults (Sun et al., 2015). Some real applications of HPT have been documented in the literature for a field of three wells penetrating a heterogeneous aquifer (Renner & Messar, 2006, Fokker et al., 2013); single and multilayer reservoirs (Rochon et al., 2008); a gas storage field confined by a lateral aquifer (Salina Borello et al., 2017), a horizontal well in a gas storage field (Fokker et al., 2018) and a geothermal system (Salina Borello et al., 2019).

Harmonic Pulse Testing involves the imposition of regular alternation of two rate values in a well, called Pulser. Combinations of different productions and/or injections or production/injection alternated with well shut-in, are possible. The effect is a pressure response that is also periodic. Then the harmonic components in both the rate and the pressure are determined through Fourier analysis, possibly preceded by pressure detrending (Viberti, 2016; Viberti et al., 2018). The pressure-rate relationship depends on the physics of the reservoir response and the parameters in the physical correlations. When the proper models are used, interpretation of measured pressure response through an inversion or parameter estimation technique can be applied to derive the reservoir properties. In this paper, we will apply the interpretation approach presented by Fokker et al. (2018) based on the strong similarity existing between the derivative of the harmonic response function versus the harmonic period and the pressure derivative versus time, typical for conventional well testing.

A great advantage of HPT is that it requires neither the initial static conditions (well shut-in of the tested well), nor the shut-in of any neighbor wells during the test. In fact, under the assumption of linearity the pressure and flow solution of a reservoir with many wells and changing production rates can then be added to the solution of the harmonic test. A Fourier transformation will pick out the signal present in the imposed frequency. Furthermore, there will be no frequency mixing; frequencies can be treated independently.

The general solution to the diffusivity equation that describes flow in a radially symmetric system, for periodic imposed injection rates, can be formulated analytically. Taking harmonic formulations for the injection rate and for the pressure; $q_{well} = q_\omega e^{i\omega t}$ and $p_\omega(\mathrm{r}, t) = g_\omega(\mathrm{r})e^{i\omega t}$, we have the general solution

$$g_\omega(r) = q_\omega C_K K_0(\zeta r) + q_\omega C_I I_0(\zeta r) \tag{1}$$

where $\zeta = \sqrt{\frac{i\omega}{\eta}}$; $\omega = 2\pi/T$ the harmonic frequency; $\eta = \frac{\lambda}{\phi c}$ is the diffusivity and $\lambda = \frac{k}{\mu}$ is the mobility, ϕ is the rock porosity, c is the total compressibility, k is the rock permeability, μ is the fluid viscosity. C_K and C_I are free parameters to be determined by imposing boundary conditions, including skin and wellbore storage. The Bessel functions have a complex argument since the differential equation has a complex parameter. As a result, the solution is complex as well, and has an amplitude and a phase when translated to the real domain.

When we consider a composite system of two concentric zones around the wellbore with different temperature, the different temperatures imply different fluid viscosities and possibly different compressibilities. Therefore the mobility (λ) the diffusivity (η) and the associated multiplier (ζ) for the radial distance is different in the two zones. The parameters and Bessel function evaluations depend on the reservoir and fluid parameters, the fluid front position, and the frequency.

From the result we can determine a response function representative of the harmonic pressure response to every harmonic component of the injection or production rate. The response function of the pulser well reads:

$$R_\omega^{pulser} = \frac{p_{well}}{q_{well}} = C_K K_0(\zeta_1 r_w) + C_I I_0(\zeta_1 r_w) + S\zeta_1 r_w \left[C_K K_1(\zeta_1 r_w) - C_I I_1(\zeta_1 r_w)\right] \tag{2}$$

3 VALIDATION OF RADIAL COMPOSITE MODEL

We validated the radial composite model for thermal front monitoring in an axially symmetric setting. A cooled zone around the injector of a geothermal doublet in a homogeneous reservoir was selected, assuming the producing well is far enough not to influence the shape of the thermal front. Two validation scenarios for thermal front monitoring were considered: case 1, after one month of injection, case 2, after six months of injection. Validation of the methodology was carried out imposing a HPT rate history (Table 2) at the end of each case. Table 1 reports the simulation parameters.

The temperature front dynamic propagation was simulated adopting an in-house single active well numerical simulator for fluid dynamics in porous media accounting for thermal effects (Verga et al., 2008, 2011, 2014). The resulting temperature profiles are shown in Figure 1. The thermal front, calculated as the distance at which the temperature reaches the average value between injection and reservoir temperature (60 °C in the considered validation cases) is 22 m for case 1 and 52 m for case 2 (Figure 1).

To calculate the synthetic response of the test, a commercial simulator was adopted. This simulator is not equipped with a thermal model, therefore a radial composite model was deployed that mimicked the thermal front with a mobility ratio representative for the thermal profile obtained from the first step. Furthermore, a sampling rate of 10 sec was imposed. The influence of possible pressure fluctuations were simulated by adding Gaussian noise of 0.04 bar (~0.02%).

The synthetic output of the pressure gauge in case 2 is shown in Figure 2. Results from the Fourier transformation of the output and a comparison with theoretically derived curves with our analytic approach are presented in Figure 3. A clear distinction is observed between the 1-month and the 6-month injection, indeed allowing for the discrimination of the thermal front.

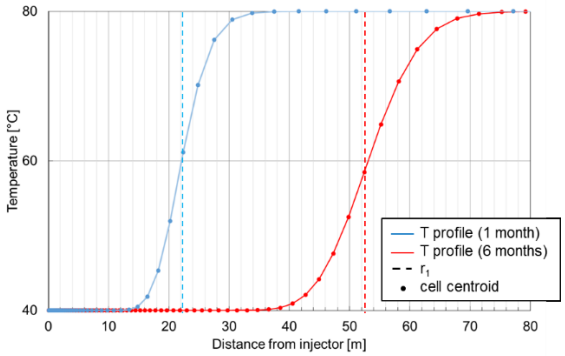

Figure 1: Numerically simulated thermal profiles at the end of 1-month pre-injection (light blue) vs at the end of 6 months of pre-injection (red) and corresponding radial composite radii.

Table 1: Simulation parameters for well, rock and water for the validation scenario

Aquifer data	
permeability (mD)	60
porosity (-)	0.2
Temperature (°C)	80
pressure (bar)	200
depth (m ssl)	2000
Net Pay (m)	100
Well	
rw (m)	0.1
S (-)	2
Rock	
compressibility (bar-1)	2.00E-05
thermal conductivity (W/K m)	2
heat capacity (J/kg K)	850
density (kg/m3)	2600
Water	
compressibility (bar-1)	4.00E-05
thermal conductivity (W/K m)	0.6
heat capacity (J/kg K)	4148
salinity (ppm)	1000
density (kg/m3)	1001
viscosity (mPa s) @ res temperature	0.34
viscosity (mPa s) @ inj temperature	0.66
injection temperature (°C)	40

Table 2: Rate history of validation scenarios

Scenario	Test	Duration/period (days)	Rate (m^3/min)	Rate variation (m^3/min)	number of periods (-)
case 1	injection operations	30	2	-	-
	HPT1	1	1.5	± 1	5
case 2	injection operations	180	2	-	-
	HPT2	1	1.5	± 1	5

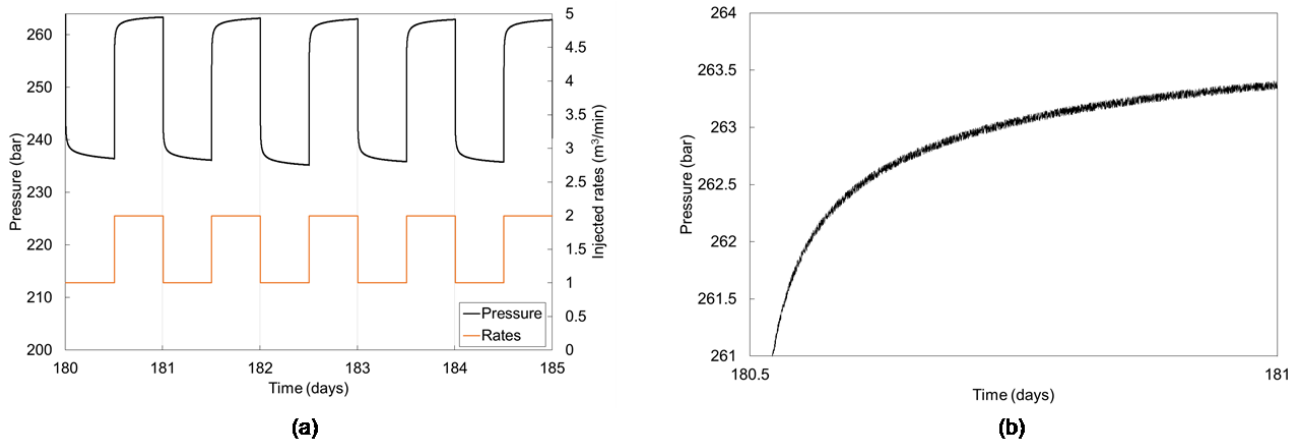

Figure 2: Noisy gauge pressures as generated by the analytic radial composite model (case 2) (a) full 5-period duration, and (b) zoom.

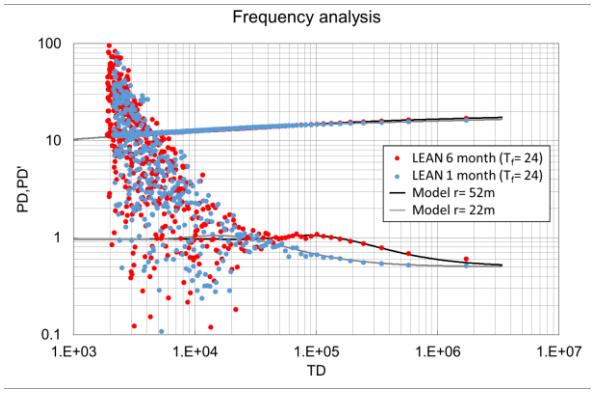

(a) (b)

Figure 3: Harmonic test frequency analysis

4. NUMERICAL MODEL OF ATES

Storage cycles were simulated through a 3D fluid-dynamic reservoir model taking into account of thermal phenomena implemented adopting a commercial software for reservoir dynamic modelling.

Well, rock and water properties of the simulated aquifer are reported in Table 3. The annual heat storage cycle rate histories are reported in Table 4.

The injection layer in the aquifer has a large horizontal permeability k_h=10760 mD, porosity ϕ = 0.37 and 30 m thickness. A significant grid refinement (cells of 4m x 4m) was imposed in an area of about 900 m x 900 m containing the wells, with the double aim of correctly simulate the pressure gauge response and accurately describe the thermal front. Grid size is then increased to 20 m x 20 m and finally to 200 m x 200 m. The initial temperature of the layer is 20°C.

HPTs were simulated at significant stages of storage cycles in order to generate synthetic data to verify the capability of the test in monitoring the heat front. More in details, the thermal front was monitored after the 5thsummer of storage (4 complete storage cycles) and after the subsequent winter and again after the 15thsummer of storage (14 complete storage cycles). Test histories are reported in Table 5. Pressure and rate data are shown in Figure 4. Expecting the thermal front to remain quite stable during the autumn and spring

periods, each test was conducted after a shut in period of one day. The adopted sampling resolution was $\Delta t = 1$ s, because preliminary synthetic tests shows that with $\Delta t > 1$ the first stabilization is hardly detectable, due to the extremely high horizontal permeability.

Table 3: Simulation parameters for well, rock and water

Well	
rw (m)	0.7874
S (-)	0
Rock	
compressibility (bar^{-1})	2.18E-05
thermal conductivity (W/K m)	2.4
heat capacity (J/kg K)	850
density (kg/m3)	2100
Water	
compressibility (bar^{-1})	4.00E-05
thermal conductivity (W/K m)	0.6
heat capacity (J/kg K)	4148
salinity (ppm)	20000
density (kg/m^3)	1016
viscosity (mPa s) @ res T	1.13
viscosity (mPa s) @ inj T	0.338
injection temperature (°C)	90

Table 4: Annual heat storage cycle

	duration (days)	Rate Well0 (m3/day)	Rate Well1 (m3/day)
summer	90	-3888	3888
Autumn	60	0	0
Winter	150	2328	-2328
Spring	60	0	0

Table 5: HPT tests for heat front monitoring on Well 0.

HPT Test	Monitoring time	Period duration (h)	Rate 1 (m3/day)	Rate 2 (m3/day)	Number of periods (-)
HPT1	after 5^{th} summer	6	1396.8	0	5
HPT2	after 5^{th} winter	6	1396.8	0	5
HPT3	after 15^{th} summer	6	1396.8	0	5

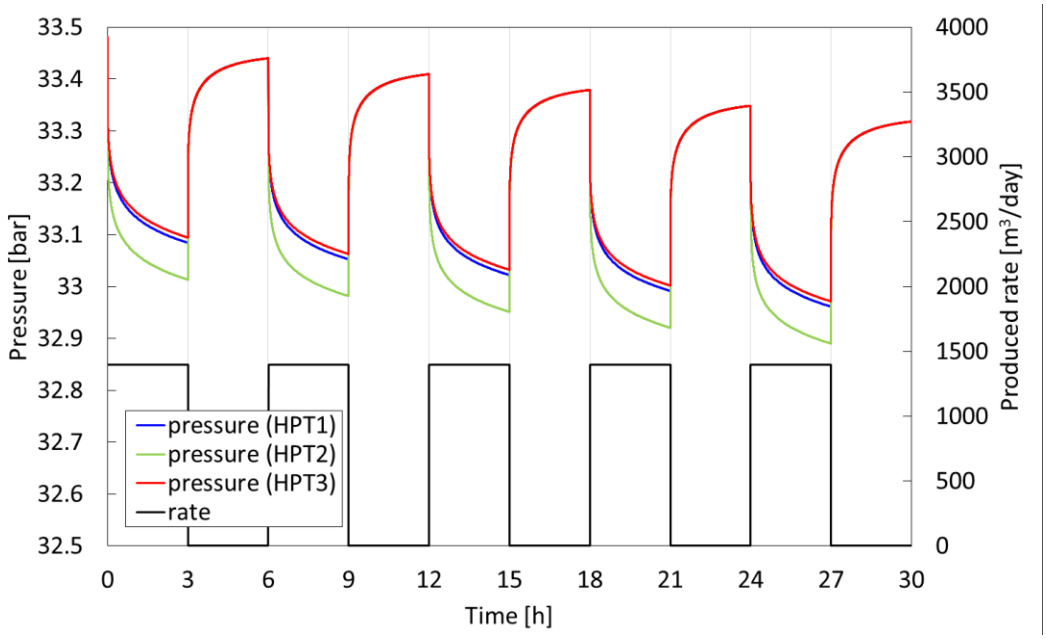

Figure 4: Simulated HPTs pressure data at tested well (Well0).

5. RESULTS

5.1 Numerical Model

In the after-summer scenario of the 5thstorage cycle (Figure 5), the simulated temperature changes gradually, but not linearly, from almost the injection temperature (90°C) to a front value (about 60°C), beyond which an abrupt change towards the initial aquifer temperature (20°C) is observed. Notice that, due to the simultaneous production in Well1, the heated zone is off-centered with respect to Well 0; it elongates toward the producing Well 1 (Figure 5, blue line). After seven months, in the after winter scenario, the situation is significantly different. The temperature around Well 0 has decreased to 50-70°C and the heated zone extension has decreased too due to the cold water injection at Well 1 (Figure 5, green line). With the progression of seasonal cycles, the after-summer heated zones tend to expand (Figure 5, red line vs. blue line).

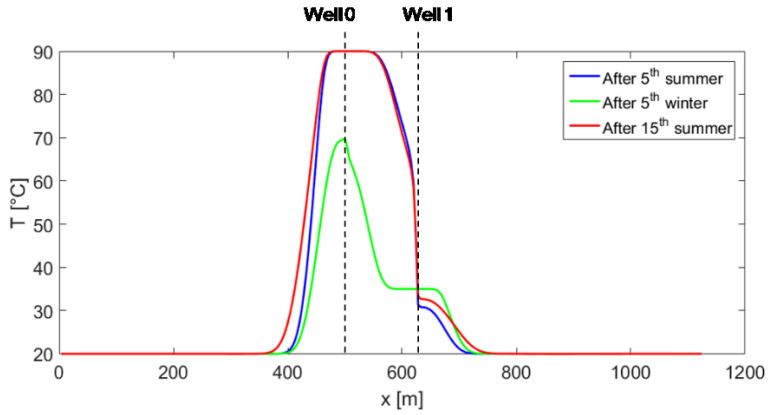

Figure 5: Temperature distributions along the x-directrix crossing the two wells.

5.2 Interpretation of HPTs

The pressure trends of the simulated HPTs were analyzed in the frequency domain. To this end, first of all rate and well pressure data were transformed through FFT obtaining Q_ω and P_ω, respectively, which represent the signal value of each frequency component $f = \omega/2\pi$. Amplitude peaks, representative of harmonics, were identified on the rate spectrum, and subsequently extracted from the rate and pressure spectrums. Then, the response function was calculated as the amplitude ratio $R_\omega = P_\omega / Q_\omega$, for each frequency component. The derivative of the amplitude ratio with respect to the logarithm of the oscillation period (R') was calculated by a three point data

differentiation algorithm (Bourdet, 2002). Log-log plots of the moduli of R and R' versus oscillation period ($2\pi/\omega$) are shown in Figure 6. Finally, the R and R' log-log plot was interpreted with our radial composite model in the frequency domain (eq. 7) to give an estimate of the extension of inner zone radius (r_1) and of the mobility ratio between inner and outer zone (M). Assuming the permeability to be constant and homogeneous, the mobility ratio represents the ratio of viscosities in the outer and the inner zone. Knowledge on the relationship between viscosity and temperature behavior then leads to an estimate of the inner zone average temperature (T_1).

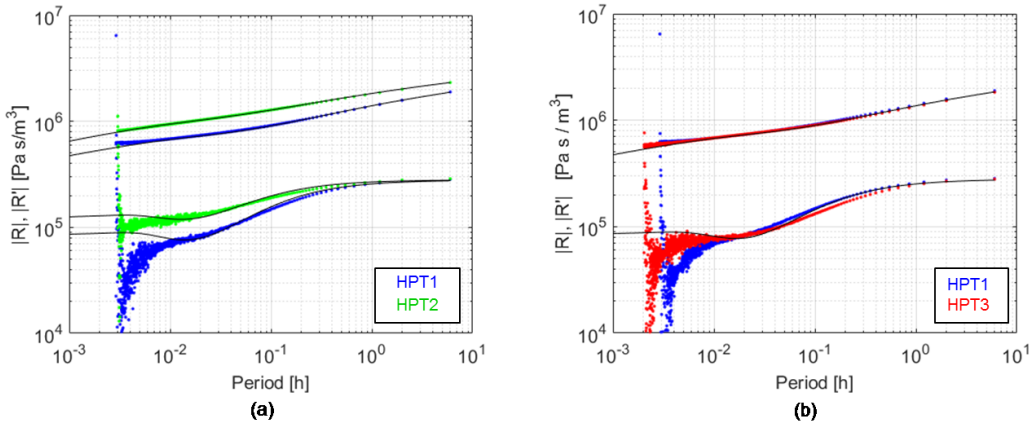

Figure 6: HPT results: (a) comparison between pressure and pressure derivative after summer (blue) vs. after winter (green) of the 5th storage cycle; (b) comparison between pressure and pressure derivative after summer of the 5th storage cycle (blue) vs. 15th storage cycle (red).

For all the tests (Figure 6), the second stabilization allowed to correctly identify a permeability value in the range 10700-10900 mD and a null skin value. Comparing after-summer and after winter-derivatives (Figure 6a), a significantly different first stabilization is observable, which corresponds to a different near-wellbore viscosity. The extent of the near-wellbore heated zone indicated by the after-summer derivative is also significantly larger than the extent indicated by the after-winter derivative. When comparing the derivatives of tests conducted after-summer of the 5th and of the 15th storage cycle (Figure 6b), the level of the first stabilization is practically the same, indicating similar temperature, but a difference is observed for the extent of the heated zone. The size is slightly larger after the summer of the 15th cycle. Values of the extent and the average temperature of the heated zone as obtained from the analytical interpretation of the three scenarios are shown in Table 6. An approximation of the temperature and the size of the heated zone calculated through numerical simulation and converted to an equivalent circumference centered in Well 0 is also given in Table 6.

Table 6: Tests interpretation results with radial composite model in the frequency domain compared with the approximation of the simulated heated zone to an equivalent circumference centered in Well 0.

Monitoring time	Radial composite HPT interpretation			Numerical simulation		
	$M = \mu_2/\mu_1$	T_1 (°C)	r_1 [m]	heated zone [°C]	T_m [°C]	r_{eq} [m]
after 5th summer	3.1	84	68	55°-90°C	83.4°C	69.8
after 5th winter	2.1	58	55	45°-70°C	55.9 C°	50.9
after 15th summer	3.1	84	75	55°-90°C	80°C	78.9

6. CONCLUSIONS

To correctly design and perform a HPT test for heat zone monitoring some features must be considered. The magnitudes of the two alternated rates are not crucial, whereas rate duration and pressure sampling are (Salina Borello et al., 2017). In particular, the test reliability is strongly related to the precision in the rate change timing. Acceptable errors in timing should be properly evaluated case by case in the test design phase and communicated to the operator who will follow the test procedure.

To make the test interpretable, the first and the second stabilization, representative of the heated zone and the undisturbed zone, respectively, must be clearly detectable on the log-log plot. Thus, in first place, the duration of the fundamental oscillation period (i.e. the sum of the duration of the two alternating constant rates) should be long enough to investigate the undisturbed zone. In the presented ATES case, being the permeability extremely high, an oscillation period $T_f \geq$ 6h (3h+3h) is sufficient to capture the stabilization corresponding to undisturbed conditions. Considering that 5 oscillations are required (Salina Borello et al., 2017), the total test duration

is 30 h, which is compatible with the storage operations. If on the one hand the high permeability reduces the required test duration, on the other hand it requires a higher precision in the test execution and a higher pressure sampling. In fact, in the log-log plot adopted for test interpretation, the first stabilization, representative of heated zone, is investigated by high frequency components corresponding in the presented ATES case to oscillation period in the range 0.003- 0.03h (from 10 s to less than 2 min). To be able to capture such information, the HPT test must be performed with extremely precise rate changes (maximum acceptable move-ups/delays 10 s). Moreover, the gauge pressure sampling must be close enough (i.e. ≥1s). These two conditions are effectual to obtain a clean pressure derivative in the periods of interest.

Under the abovementioned conditions, results show that HPT interpretation with the presented radial composite model provides reliable information and can be successfully applied to monitor Aquifer Thermal Energy Storage. It is remarked that the obtained information does not exactly reproduce the thermal front. In particular radial composite model is not able to correctly predict the front position in between the two wells. In fact, due to the contemporary injection/production in Well1, the heated zone is not centered in Well0, neither circular. However, the test interpretation gives valuable information about average heated zone extension and temperature and allows to monitor its changes during the storage cycle and over the years, thus enabling eventual adjustment of the cycle history over the years.

REFERENCES

Ahn, S., & Horne, R.N. (2010). Estimating permeability distributions from pressure pulse testing. In Proceedings - S*PE Annual Technical Conference and Exhibition*, 3:2388-2403. Florence. https://doi.org/10.2118/134391 - MS.

Black, J. H., & Kipp, K. L. J. (1981). Determination of hydrogeological parameters using sinusoidal pressure tests: A theoretical appraisal. *Water Resources Research*, 17(3), 686-692. https://doi.org/10.1029/WR017i003p00686.

Bourdet, D. (2002). Well west analysis: The Use of Advanced Interpretation Models: Handbook of Petroleum Exploration and Production, 3. Amsterdam: Elsevier Science B.V. ISBN: 978 - 0 - 444 - 54988 - 4.

Cardiff, M., Bakhos, T., Kitanidis, P. K., & Barrash, W. (2013). Aquifer heterogeneity characterization with oscillatory pumping: Sensitivity analysis and imaging potential. *Water Resources Research*, 49, 5395-5410. https://doi.org/10.1002/wrcr.20356.

Cardiff, M., & Barrash, W. (2015). Analytical and semi - analytical tools for the design of oscillatory pumping tests. *Groundwater*, 53(6), 896-907. https://doi.org/10.1111/gwat.12308.

Chen, Y., & Renner, J. (2018). Exploratory use of periodic pumping tests for hydraulic characterization of faults. *Geophysical Journal International*, 212(1), 543-565. https://doi.org/10.1093/gji/ggx390.

Copty, N. K., & Findikakis, A. N. (2004). Stochastic analysis of pumping test drawdown data in heterogeneous geologic formations [Analyse stochastique des données de rabattement obtenues en pompages d'essai dans des formations géologiques hétérogènes]. *Journal of Hydraulic Research*, 42(sup1), 59-67. https://doi.org/10.1080/00221680409500048.

Despax, D., Dovis, R., Fedele, J. - M., & Martin, J. - P. (2004). Method and device for determining the quality of an oil well reserve. U.S. Patent, 6, 801-857.

Fokker, P. A., Renner, J., & Verga, F. (2013). Numerical modeling of periodic pumping tests in wells penetrating a heterogeneous aquifer. *American Journal of Environmental Sciences*, 9(1), 1-13. https://doi.org/10.3844/ajessp.2013.1.13.

Fokker, P. A., Salina Borello, E., Serazio, C., & Verga, F. (2012). Estimating reservoir heterogeneities from pulse testing. *Journal of Petroleum Science and Engineering*, 86 - 87, 15-26. https://doi.org/10.1016/j.petrol.2012.03.017.

Fokker, P. A., Salina Borello, E., Verga, F., & Viberti, D. (2018). Harmonic pulse testing for well performance monitoring. *Journal of Petroleum Science and Engineering*, 162, 446-459. https://doi.org/10.1016/j.petrol.2017.12.053.

Fokker, P. A., & Verga, F. (2011). Application of harmonic pulse testing to water - oil displacement. *Journal of Petroleum Science and Engineering*, 79(3-4), 125-134. https://doi.org/10.1016/j.petrol.2011.09.004.

Gringarten A.C., (2008) From Straight Lines to Deconvolution: The Evolution of the State of the Art in Well Test Analysis. SPE Reservoir Evaluation & Engineering - *SPE Reservoir Evaluation & Engineering*. 11(01) pp. 41-62. 10.2118/102079-PA.

Guiltinan, E., & Becker, M. W. (2015). Measuring well hydraulic connectivity in fractured bedrock using periodic slug tests. *Journal of Hydrology*, 521, 100-107. https://doi.org/10.1016/j.jhydrol.2014.11.066.

Hollaender, F., Hammond, P. S., & Gringarten, A. C. (2002). Harmonic testing for continuous well and reservoir monitoring. In Proceedings - *SPE Annual Technical Conference and Exhibition*, (pp. 3071-3082). San Antonio, TX: Society of Petroleum Engineers (SPE). https://doi.org/10.2118/77692 - MS.

Kuo, C. H. (1972). Determination of reservoir properties from sinusoidal and multirate flow tests in one or more wells. *Society of Petroleum Engineers Journal*, 12(06), 499‐507. https://doi.org/10.2118/3632‐PA.

Morozov, P. E. (2013). Harmonic testing of hydraulically fractured wells. *Proceeding of 17th European Symposium on Improved Oil Recovery*. St. Petersburg, Russia, 16‐18 April 2013.

Renner, J., & Messar, M. (2006). Periodic pumping tests. *Geophysical Journal International*, 167(1), 479–493. https://doi.org/10.1111/j.1365-246X.2006.02984.x.

Rochon, J., Jaffrezic, V., De La Combe, J.L.B., Azari, M., Roy, S., Dorffer, D., et al. (2008). Method and application of cyclic well testing with production logging. In Proceedings ‐ *SPE Annual Technical Conference and Exhibition*, 4:2376‐90. Denver, CO. https://doi.org/10.2118/115820‐MS.

Rosa, A. J., & Horne, R. N. (1997). Reservoir description by well‐test analysis by use of cyclic flow‐rate variation. *SPE Formation Evaluation*, 12(04), 247‐254. https://doi.org/10.2118/22698‐PA.

Salina Borello, E., Fokker, P. A., Viberti, D., Espinoza, R., & Verga, F. (2017). Harmonic‐pulse testing for non‐Darcy‐effects identification. *SPE Reservoir Evaluation and Engineering*, 20(02), 486‐501. https://doi.org/10.2118/183649‐PA.S.

Salina Borello, E., P.A. Fokker, D. Viberti, F. Verga, H. Hofmann, P. Meier, K.-B. Min, K. Yoon, and G. Zimmermann. (2019) "Harmonic Pulse Testing for Well Monitoring: Application to a Fractured Geothermal Reservoir." *Water Resources Research*, 2019. 2018WR024029. https://doi.org/10.1029/2018WR024029.

Sun, A. Y., Lu, J., & Hovorka, S. (2015). A harmonic pulse testing method for leakage Detection in deep subsurface storage formations. *Water Resources Research*, 51, 4263‐4281. https://doi.org/10.1002/2014WR016567.

Verga, F., Viberti, D., & Salina Borello, E. (2008). A new 3‐D numerical model to effectively simulate injection tests. *In 70th European Association of Geoscientists and Engineers Conference and Exhibition 2008: Leveraging Technology. Incorporating SPE EUROPEC 2008* (Vol. 2, pp. 946‐959). Rome: Society of petroleum engineers. https://doi.org/10.2118/113832‐MS.

Verga, F., Viberti, D., Salina Borello, E., & Serazio, C. (2014). An effective criterion to prevent injection test numerical simulation from spurious oscillations. *Oil & Gas Science and Technology* ‐ Revue d'IFP Energies Nouvelles, 69(4), 633–651. https://doi.org/10.2516/ogst/ 2013137.

Verga F., Viberti D., Salina Borello E: (2011). A new insight for reliable interpretation and design of injection tests. *Journal of Petroleum Science and Engineering* **78**(1) (2011) 166–177 Elsevier. doi 10.1016/j.petrol.2011.05.002.

Viberti, D. (2016). Effective detrending methodology for harmonic transient pressure response. *Geoingegneria Ambientale e Mineraria*, 149(3), 55‐62.

Viberti, D., Salina Borello, E., & Verga, F. (2018). Pressure detrending in harmonic pulse test interpretation: When, why and how. *Energies*, 11(6), 1540 MDPI. https://doi.org/10.3390/en11061540.

Vinci, C., Steeb, H., & Renner, J. (2015). The imprint of hydro‐mechanics of fractures in periodic pumping tests. *Geophysical Journal International*, 202(3), 1613‐1626. https://doi.org/10.1093/gji/ggv247.